DOI: 10.26599/FSHW.2024.9250026

Contents lists available at SciOpen

Food Science and Human Wellness

journal homepage: https://www.sciopen.com/journal/2097-0765

Improvement of *Lactiplantibacillus plantarum* MWFLp-182 on oxidative deficits induced by in 2,2'-azobis(2-methylpropionamidine) dihydrochloride and the relating key gene analysis

Hui Nie[a,b], Xutong Ma[a,b], Fanyu Kong[a,b], Yanghe Luo[c], Guangqing Mu[a,b,*], Xiaomeng Wu[a,b,*]

[a] *School of Food Science and Technology, Dalian Polytechnic University, Dalian 116034, China*

[b] *Dalian Probiotic Function Research Key Laboratory, Dalian Polytechnic University, Dalian 116034, China*

[c] *Guangxi Key Laboratory of Health Care Food Science and Technology, Hezhou University, Hezhou 542899, China*

ABSTRACT: *Lactiplantibacillus plantarum* MWFLp-182 was originally isolated from the feces of long-living elderly individuals in Hezhou city, Guangxi, China. *L. plantarum* MWFLp-182 showed favorable gastric and intestinal tolerance compared with *Lactiplantibacillus rhamnosus* GG (LGG). *L. plantarum* MWFLp-182 was further examined for its antioxidant and anti-inflammatory activity in ABAP-treated HT-29 cells. Importantly, it enhanced the expression of anti-inflammatory factor (interleukin-10 (IL-10)), antioxidant cytokines (superoxide dismutase (SOD), glutathione peroxidase (GPx), nuclear factor erythroid 2-related factor (Nrf2), and hemeoxygenase 1(HO-1)), B-cell lymphoma-2 (Bcl-2), and tight junction (Zonula occludens protein 1(ZO-1), Claudin-1, and Occludin) proteins and genes, and reduced reactive oxygen species (ROS). The complete genome of *L. plantarum* MWFLp-182 contained a single circular chromosome that was 3 257 196 bp long, with a G + C content of 44.49%, and a single circular plasmid that was 53 560 bp long. The genes *tpx*, *trxA*, *trxB*, *npr*, *nrdH*, *dps*, *recA, gpx*, *gshA* and *arsC* in this strain were related to antioxidant function; the key genes involved in antioxidant function were further investigated. In this study, we identified a probiotic candidate with antioxidant properties.

Keywords: *Lactiplantibacillus plantarum*; Antioxidant strain; Complete genome sequence

1. Introduction

With societal development, health and longevity of the elderly have attracted considerable attention in recent years. Older adults tend to be afflicted with a series of diseases such as Alzheimer's and Parkinson's diseases[1]. This is mainly due to aging of the body, reduced cellular protection mechanisms, and increased intracellular content of reactive oxygen species (ROS). An increase in ROS activity leads to oxidative stress and the production of free radicals such as superoxide anions, hydroxyl radicals, and transition metals[2]. Oxidative stress is accompanied by a series of genetic, cellular, and epigenetic changes that damage the body[1,3]; thus, oxidative stress plays a role in the development of chronic diseases such as diabetes, heart disease, rheumatoid arthritis, and aging[4-5]. However, oxidative stress may be inhibited by antioxidant enzymes such as superoxide dismutase (SOD), glutathione peroxidase (GPx), and catalase (CAT)[2].

***Corresponding author**
GuangqingMu@163.com (G.Q. Mu); wuxiaomeng0812@163.com (X.M. Wu)

Received 21 March 2023
Received in revised from 15 May 2023
Accepted 29 June 2023

Probiotics are defined as "live microorganisms that, when administered in adequate amounts, confer a health benefit on the host"[6]. Lactic acid bacteria (LAB) are the most common probiotics. *Lactiplantibacillus plantarum* is a Gram-positive bacterium which can be found in various sources in regular life, including in fermented food[7], paocai[8], yogurt[9], cheese[10], and the feces of humans and animals[11-14]. *L. plantarum* has been reported to demonstrate antioxidant[13], anti-inflammatory[15], antibacterial[16], anticancer[17], and anti-obesity[18] functions.

L. plantarum Y44 was isolated from fish guts and showed antioxidant activity[19]. *L. plantarum* Y42 and *L. plantarum* ZLP001 alleviated the reduction in tight junction (TJ) protein expression, downregulated the expression of proinflammatory cytokines (interleukin-6 (IL-6), tumor necrosis factor-α (TNF-α)), and upregulated the expression of anti-inflammatory cytokines (IL-10)[20-21]. While *L. plantarum* should be capable of tolerating gastrointestinal conditions (low pH, bile acids, and gastric enzymes), and adhere the gut to as probiotics[22]. *L. plantarum* FLPL05 was isolated from the feces of long-living elderly individuals and exhibited high antioxidant activity[14].

In recent years, with the rapid development of sequencing techniques, probiotic functions have been investigated using complete genome sequencing. A survey of the available research has shown that a series of whole-genome sequences of *L. plantarum* have been extensively studied[23-24]. Whole-genome sequencing has aided functional genomic studies and safety evaluations[25]. However, the function of gene excavates, especially antioxidant functions, is being revisited.

In a previous study, we analyzed the diversity of the intestinal flora of the elderly in Hezhou, Guangxi, China, and found that *Lactobacillus* belonged to the preponderance genus in the long-living elderly. We isolated 135 strains from fecal of long-living elderly individuals in Hezhou city, Guangxi, China. Interestingly, *L. plantarum* MWFLp-182 showed the highest antioxidant activity and great safety features showed in **Table S1.** We evaluated the antioxidant and anti-inflammatory activities of *L. plantarum* MWFLp-182 with common probiotic properties in HT-29 cells treated with 2,2'-azobis(2-methylpropionamidine) dihydrochloride (ABAP). To better understand the antioxidant mechanism used by *L. plantarum* MWFLp-182, we studied the genome of *L. plantarum* MWFLp-182 and analyzed the core and oxidative stress tolerance genes. This provides a reliable theoretical basis for the subsequent identification of genes that regulate antioxidant functions and for high-throughput sequencing.

2. Materials and methods

2.1. Bacterial strain, culture conditions, and DNA extract

L. plantarum MWFLp-182 was originally isolated from the feces of long-living elderly individuals in Hezhou city, Guangxi, China, and stored at the Dalian Probiotic Function Research Key Laboratory, Dalian Polytechnic University (China). It was maintained in de Man, Rogosa, and Sharpe (MRS) medium (AOBOX Biotechnology, Qingdao, China) at 37 ℃ for (16−18) h under aerobic conditions. Bacterial cells were collected through centrifugation at 6 000 × *g* for 5 min at room temperature. Bacterial DNA was extracted using the E.Z.N.A.® Soil DNA Kit (Omega Biotek, Norcross, GA, USA) according to the manufacturer's

instructions. The concentration and purity of the extracted DNA were determined using a TBS-380 fluorometer (Turner BioSystems Inc., Sunnyvale, CA, USA), and the DNA samples with $A_{260\,nm}$/ $A_{280\,nm}$ ratios of approximately 1.80−2.00 were used for further experiments[26].

2.2. Whole-genome sequencing and genome annotation

The genomic DNA of *L. plantarum* MWFLp-182 was sequenced using a combination of the PacBio RS II Single Molecule Real-Time (SMRT) and Illumina sequencing platforms. Genomic DNA of 1 μg was used per strain for sequencing library construction. DNA samples were sheared into (400−500) bp fragments using a Covaris M220 Focused Acoustic Shearer following the manufacturer's protocol. Illumina sequencing libraries were prepared from the sheared fragments using a NEXTflex Rapid DNA-Seq Kit. All analyses were performed using the free online Majorbio Cloud Platform (https://www.majorbio.com) from Shanghai Majorbio Biopharm Technology Co., Ltd. The original image data were transformed into sequence data via base calling, which was defined as raw data or raw reads, and then saved as a FASTQ file. Subsequently, the reads were assembled into contigs using the hierarchical genome assembly process (HGAP) and Canu[27]. Glimmer[28] was used for coding sequence (CDS) prediction. The predicted CDSs were annotated using the NR, latest version; Swiss-Prot, Version 2017.04.10; Prom Predict; Cluster of Orthologous Groups of proteins (COG) and Kyoto Encyclopedia of Genes and Genomes (KEGG)[29] databases. In total, 7 040 340 paired-end reads were obtained.

2.3 Auto-aggregation assay

Auto-aggregates were prepared according to the method described by Liu et al.[30], with minor modifications. *L. plantarum* MWFLp-182 and *Lactiplantibacillus rhamnosus* GG (LGG) were cultured for (16−18) h and harvested by centrifugation (4 000 × *g*, 5 min). The sediment was washed thrice with saline and adjusted to 10^9 CFU/mL. *L. plantarum* MWFLp-182 and LGG were incubated at 37 ℃ for 24 h. The optical density (OD) of the culture medium at 600 nm was measured at 0, 2, 4, 6, 12, and 24 h using an enzyme-labeled instrument (Thermo Scientific Multiskan GO). Each test was performed in triplicate. Auto-aggregation ability was calculated as Eq (1).

$$\text{Auto-aggregation ability (\%)} = (1 - A_t/A_0) \times 100 \quad (1)$$

where, A_t is $OD_{600\,nm}$ at 2, 4, 6, 12 and 24 h; A_0 is $OD_{600\,nm}$ at 0 h.

2.4 Co-aggregation assay

Co-aggregation analysis of *L. plantarum* MWFLp-182 was performed according to the method described by Liu et al.[30] with minor modifications. *L. plantarum* MWFLp-182 and *Salmonella* (ATCC 14028) were cultured for (16−18) h and harvested using centrifugation (4 000 × *g*, 5 min). The sediment was washed thrice with physiological saline and adjusted to an OD of (0.50 ± 0.05). Equal volumes (3 mL) of *L. plantarum* MWFLp-182 together with pathogenic *Salmonella* cell suspensions were mixed by vortexing for 5 min and incubated at 37 ℃ for 24 h. The OD at 600 nm of the culture medium was measured at 0, 2, 6, 10, and 24 h, using an enzyme-labeled instrument (Thermo Scientific Multiskan GO). Co-aggregation ability was calculated as Eq (2).

Co-aggregation ability (%) = $(A_1 + A_2 - 2A_{12})/(A_1 + A_2) \times 100$ (2)

where, A_1 and A_2 represent absorbance of the LAB at 0 h, respectively; A_{12} represent absorbance of the mixture after 2, 6, 10 and 24 h.

2.5 Gastrointestinal tolerance assay

Gastrointestinal tolerance was evaluated according to the method described by Kingkaew et al.[31] with minor modifications. To simulate gastric fluid, gastric protease was dissolved in phosphate buffered saline (PBS) (0.1 mol/L, pH 7.3), its consistence was adjusted to 3.0 g/L (pH 2.5), and it was filtered through a sterile membrane (0.22 μm, Millex-GP). To simulate intestinal fluid, trypsin was dissolved in PBS (0.1 mol/L, pH 7.3), its consistence was adjusted to 1.0 g/L (pH 8.0), and it was filtered through a sterile membrane (0.22 μm, Millex-GP). The cells was counted using plate and colony counting method after treatment with simulated gastric fluid with the volume ratio of 1:9 at 37 ℃ for 3 h and then with simulated intestinal fluid at the same volume ratio at 37 ℃ for 8 h. Strain survival ability was calculated as Eq (3).

Strain survival ability (%) =lg N_1/lg N_0 (3)

where, N_1 represents the viable LAB count in simulated gastric or intestinal fluid; N_0 represents initial viable count of LAB.

2.6 Cell Cytotoxicity Assay

The methylene blue assay was performed as previously described by Xing et al[32]. The HT-29 cells (human colon adenocarcinoma cells) were cultured at 37 ℃ in a 5% CO_2 atmosphere in RPMI 1640 medium (Gibco Life Technologies, USA) supplemented with 10% (*V/V*) heat-inactivated fetal bovine serum (FBS) and 1% (*V/V*) penicillin-streptomycin solution. HT-29 cells were seeded in 96-well plate at a density of 4×10^4 cells/mL for 100 μL and incubated for 24 h at 37 ℃. After washing with PBS thrice, HT-29 cells were treated with 100 μL of *L. plantarum* MWFLP-182 (10^9 CFU/mL dissolved in RPMI 1640 medium (without heat-inactivated FBS)) for 24 h at 37 ℃. After washing with PBS thrice, cells were incubated with 50 μL/well methylene blue for 1 h at 37 ℃. After washing with PBS until the PBS was clear, 100 μL/well of the eluent was added. After 20 min of shock, the absorbance was measured at 570 nm. LGG was used as a positive control and RPMI 1640 medium (without heat-inactivated FBS) was used as a blank control.

2.7 Adhesion assay

The adhesion of *L. plantarum* MWFLp-182 was evaluated as described by Plessas et al[33] with minor modifications. HT-29 cells were seeded in 12-well plates at a density of 5×10^5 cells/mL in 1mL and incubated for 24 h. After washing three times with PBS, HT-29 cells were treated with 1 mL of *L. plantarum* MWFLp-182 or LGG (10^9 CFU/mL dissolved in RPMI 1640 medium (without heat-inactivated FBS)). After 3 h of co-incubation at 37 ℃, the cells were washed with PBS thrice, and lysed using 500 μL 1% Triton X-100 (Solarbio, China). Lysates were diluted in PBS, plated on MRS agar, and incubated at 37 ℃ for 36 h. The adhesion ratio was calculated as Eq (4)

Adhesion ratio (%) = $(V_1/V_2) \times 100$ (4)

where, V_2 is the initial viable cell count of *L. plantarum* MWFLp-182 or LGG. V_1 is the initial viable count of *L. plantarum* MWFLP-182 or LGG, obtained from HT-29 cells.

2.8 Measurement of intracellular ROS in HT-29 cells

As is previously known, 2,7-dichloroflurescin diacetate (DCFH-DA) is a fluorescein-labeled dye that can measure intracellular ROS[34]. HT-29 cells were seeded in a 24-well plate at a density of 1×10^5 CFU/mL cells per well at 37 ℃ for 24 h. At 85% confluence, the cells were washed three times with PBS and HT-29 cells were treated with 1 mL of *L. plantarum* MWFLp-182 (LP) or LGG (10^9 CFU/mL dissolved in RPMI 1640 medium (without heat-inactivated FBS)). After 3 h of co-incubation at 37 ℃, the cells were washed with PBS thrice, incubated with 500 μL of 110 mmol/L 2,2′-azobis (2-methylpropionamidine) dihydrochloride (ABAP) at 37 ℃ for 2 h. The cells were washed three times with PBS, and incubated with 500 μL of 10 mmol/L DCFH-DA in the dark at 37 ℃ for 30 min. Subsequently, the cells were washed twice with PBS and the fluorescence intensity was determined using fluorescence microscopy (OLYMPUS DP74, Japan) at excitation and emission wavelengths of 488 and 525 nm, receptively. Cells treated with DCFH-DA were used as blank control (denoted "K"), while cells treated with DCFH-DA and ABAP were used as a positive control (signed denoted "ABAP").

2.9 Determination of mRNA expression

The mRNA expression levels of TJ (Zonula occludens protein 1 (*ZO-1*), *Cluadin-1*, and *Occludin*), inflammatory (interleukin (*IL-1β*), *IL-6*, and *IL-10*), oxidant cytokines (superoxide dismutase 3 (*SOD3*), malonic dialdehyde (*MDA*), nuclear factor erythroid 2-related factor (*Nrf2*), hemeoxygenase 1 (*HO-1*), and glutathione peroxidase (*GPx*)), and *Bcl-2* were determined using quantitative real-time quantitative PCR (RT-qPCR). HT-29 cells were collected and lysed, and total RNA was extracted according to the manufacturer's instructions (FastPure® Cell/Tissue Total RNA Isolation Kit V2, China). RNA concentrations were determined with an ultra-micro spectrophotometer (SpectraMax® QuickDrop™, USA) and purity was verified using $A_{260\,nm}/A_{280\,nm}$ and $A_{260\,nm}/A_{230\,nm}$ absorbance ratios. RNA was reverse transcribed using a cDNA Synthesis Kit (HiScript® IIQ RT SuperMix for qPCR (+ gDNA wiper)) and qPCR was performed using ChamQ Universal SYBR qPCR Master MIX (Vazume, China) on a StepOne real-time PCR system (Thermo Fisher Scientific, Applied Biosystems, USA). Relative gene expression was calculated using the $2^{-\Delta\Delta Ct}$ method after qPCR was performed as follows: stage 1: 95 ℃ for 30 s by 1 amplification cycle; stage 2: 95 ℃ for 10 s, 60 ℃ for 30 s by 40 amplification cycles; stage 3: 95 ℃ for 15 s, 60 ℃ for 60 s, 95 ℃ for 15 s by 1 amplification cycle.

2.10 Western blot assay

ZO-1, Claudin-1, Occludin, and *β*-actin expression levels were determined according to the methods described by Ma et al[35].

2.11 Statistical analysis

All tests were performed in triplicate. Data are presented as means ± standard deviation (SD). IBM SPASS Statistics 23 was used for statistical analysis. The mRNA and protein expression levels were analyzed using one-way ANOVA to the differences between different experimental groups, and the post hoc test using least significance difference. The results were considered statistically significant at $P < 0.05$.

3. Results

3.1. Genome features and phylogenetic analysis of L. plantarum MWFLp-182

Whole-genome sequencing and comprehensive bioinformatic analysis of *L. plantarum* MWFLp-182 are shown in **Table 1 and Fig. 1**. The complete genome of *L. plantarum* MWFLp-182 was of 3 310 756 bp long with a GC content of 44.49% and contained 3 169 predicted genes, including 3 085 protein-CDS, 68 tRNAs, and 16 rRNAs. The 68 tRNA encoding sequences correspond to 21 amino acids (**Table S2**), which are alanine (Ala, 3), asparagine (Asn, 4), aspartic acid (Asp, 3), cysteine (Cys, 1), glutamine (Gln, 3), glutamic acid (Glu, 3), glycine (Gly, 6), histidine (His, 2), isoleucine (Ile, 3), leucine (Leu, 6), lysine (Lys, 4), methionine (Met, 3), phenylalanine (Phe, 2), proline (Pro, 3), serine (Ser, 4), threonine (Thr, 4), tryptophan (Trp, 1), tyrosine (Tyr, 2), valine (Val, 3), and undetected (3).

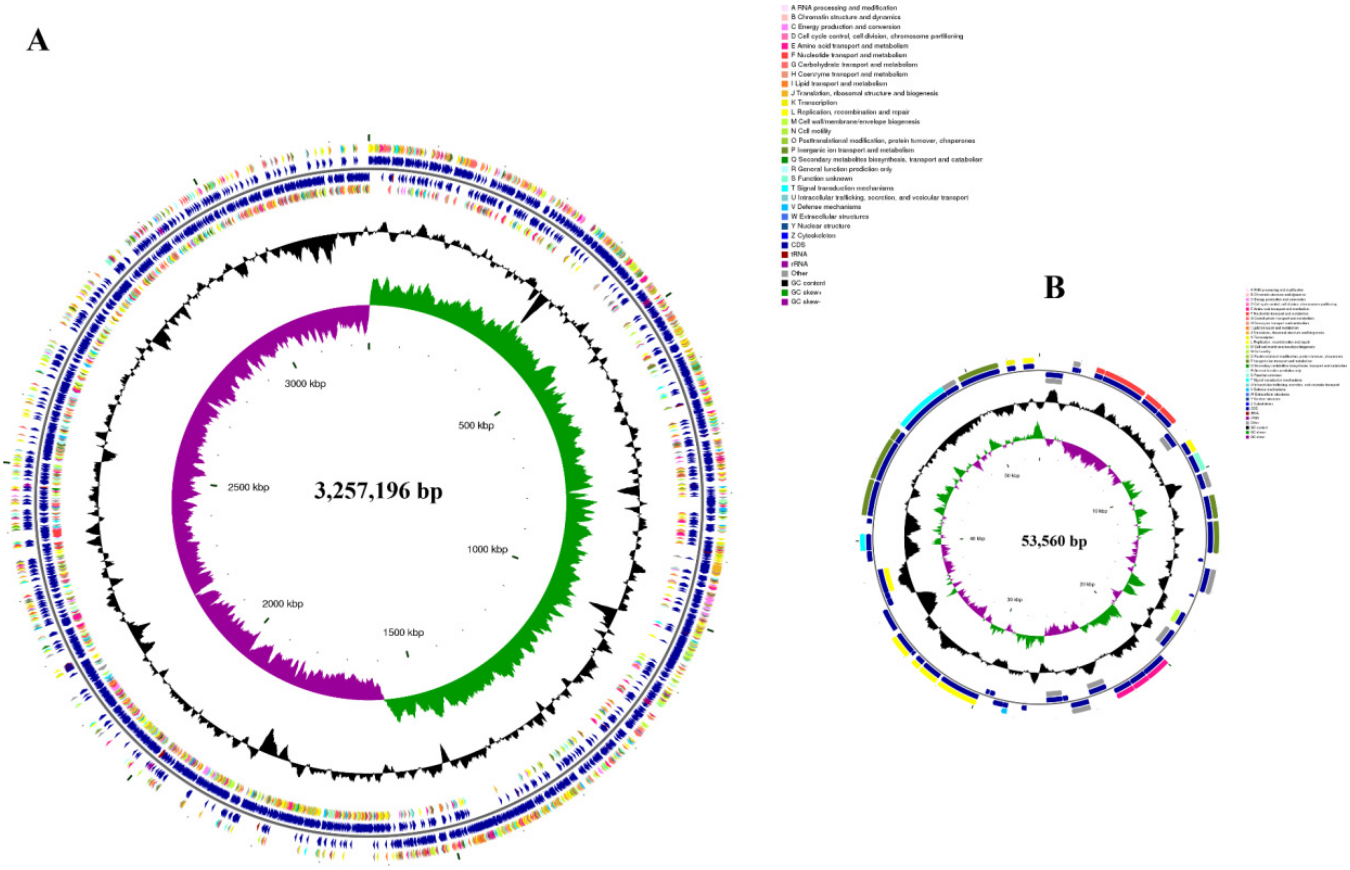

Fig. 1. General genomic attributes of *L. plantarum* MWFLp-182. (**A**) Circular map of *L. plantarum* MWFLp-182. From outside to inside Ring 1: COG annotation information in the positive strand. Ring 2: CDS annotation information in the positive strand. Ring 3: CDS annotation information in the negative strand. Ring 4: COG annotation information in the negative strand; Ring 5, 6 and 7: GC content, GC skew, and genome size, respectively. (**B**) Circular map of plasmid *L. plantarum* MWFLp-182. From outside to inside Rings 1 and 4 depicts CDS on positive and negative annotation, and different colors indicate different COG functional classification. Rings 2 and 3 depicts CDS, tRNA, rRNA on positive and negative annotation. Rings 5 depict GC content, the outward part indicates the GC content of the region is higher than the average GC content, the higher the peak is the average GC content, the higher the GC content, the higher the peak and the average GC content. Rings 6 and represents GC skew and genome size, respectively.

Table 1. *L. plantarum* MWFLp-182 genome features.

Attribute	Values
Genome size (bp)	3310756
GC content (%)	44.49
Total genes	3169
CDS (protein)	3085
tRNA genes	68
rRNA genes	16

The phylogenetic tree was constructed by selecting the closest 16 strains at the species level based on the 16S rRNA sequence, and by selecting the neighbor-joining method using MEGA 11.0 (**Fig. 2**). BLAST and average nucleotide identity (ANI) analysis of the strain showed 99.93% identity, with *L. plantarum*.

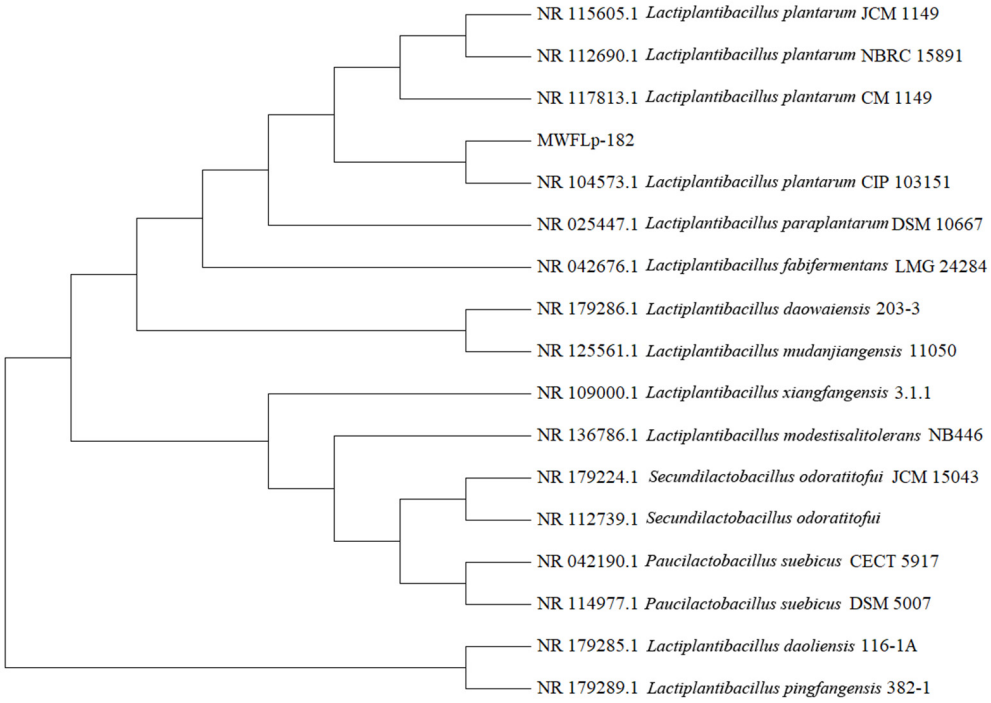

Fig. 2. Neighbor-joining phylogenetic tree of *L. plantarum* MWFLp-182 strains based on 16S rRNA genes found by MEGA (version 11.0).

3.2. Functional annotation

Well-rounded functional annotation of *L. plantarum* MWFLp-182 was performed using COG, Gene Ontology (GO), KEGG, and carbohydrate-active enzymes (CAZy) analyses of its genes/CDSs. COG is a useful database for examining the functional characteristics of sequenced genomes, and comparing microbial communities[36]. GO is a bioinformatics concept that has been widely used to study genes of all species[37]. KEGG was used to examine the metabolic pathways in *L. plantarum* MWFLp-182.

A total of 2 445 (79.25%) genes of *L. plantarum* MWFLp-182 strain were assigned to 23 COG function classifications (**Fig. 3A**). The category "garbohydrate transport and metabolism" was the most abundant (gene number: 294, 12.02%), followed by "transcription" (gene number: 282, 11.53%), "amino acid transport and metabolism" (gene number: 222, 9.08%), "general function prediction only" (gene number: 217, 8.88%), "translation, ribosomal structure and biogenesis" (gene number: 215, 8.79%). GO terms of molecular function

(gene number: 1955) were the most abundant, followed by those of cellular components (gene number: 1 188) and biological processes (gene number: 1 097) (**Fig. 3B**).

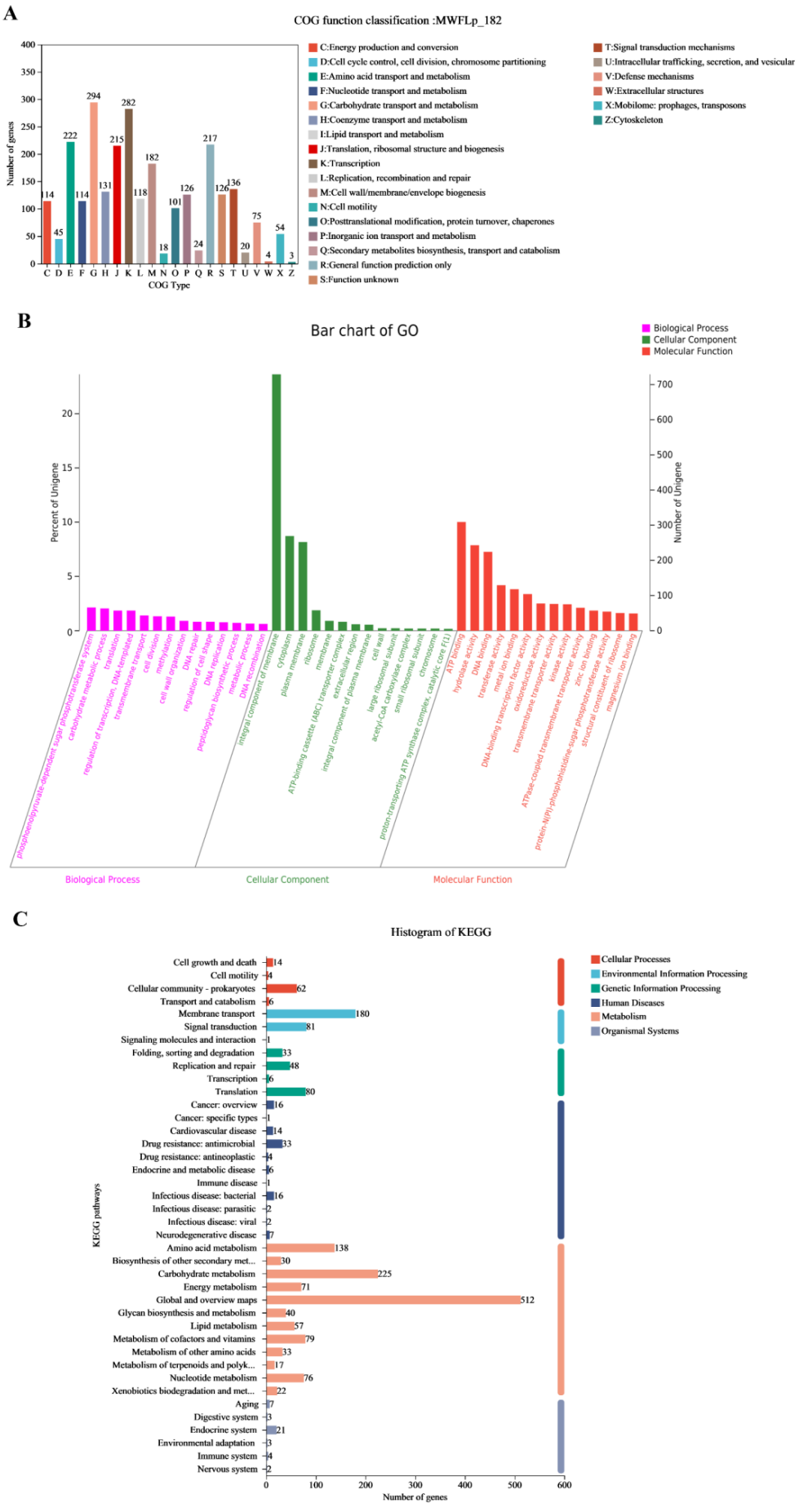

Fig. 3. (A) Functional categories of *L. plantarum* MWFLp-182 annotated by COGs. (B) GO slim classifications for *L. plantarum* MWFLp-182. (C) Gene number of KEGG.

For *L. plantarum* MWFLp-182 isolated from the feces of long-living elderly individuals, genes in the cellular component category were divided into 14 sub-functions with a large proportion in the integral components of membranes (GO: 0016021, gene number: 729, gene percent: 23.63%); genes in the molecular function category were divide into 14 sub-functions, with most involved in functions of ATP binding (GO: 0005524, gene number: 309, gene percent: 10.02%), hydrolase activity (GO: 0016787, gene number: 243, gene percent: 7.88%), and DNA binding (GO: 0003677, gene number: 224, gene percent: 7.26%); genes in biological process category were divided into 14 sub-functions, with most involved in phosphoenolpyruvate-dependent sugar phosphotransferase system (GO: 0009401, gene number: 66, gene percent: 2.14%), carbohydrate metabolic process (GO: 0005975, gene number: 63, gene percent: 2.04%), translation (GO: 0006412, gene number: 57, gene percent: 1.85%), and regulation of transcription, DNA-templated (GO: 0006355, gene number: 57, gene percent: 1.85%). *L. plantarum* MWFLp-182 CDSs (52.74%) were assigned to 6 (First Category) and 40 KEGG pathways (second category) (**Fig. 3C**). The category “global and overview maps” was the most abundant (gene number: 512), followed by “carbohydrate metabolism” (gene number: 225), “membrane transport” (gene number: 180), and “amino acid metabolism” (gene number: 138).

CAZy can be used to classify the functions of carbohydrate-active enzymes. We analyzed the CAZymes in *L. plantarum* MWFLp-182 genomes, which contained 110 genes, including four CAZymes gene classes: 33 glycosyl transferase genes (GT), 11 auxiliary activities genes (AA), 48 glycoside hydrolase genes (GH), and 18 carbohydrate esterase genes (CE) (**Table S3**).

3.3 Adhesion capacity, Auto-aggregation, co-aggregation, and gastrointesinal tolerance assay

The adhesion capacity of *L. plantarum* MWFLp-182 was similar to that of LGG (**Fig. 4A**). HT-29 cell survival rate was greater than 90% after treatment with *L. plantarum* MWFLp-182 or LGG (**Fig. 4B**). Thus, *L. plantarum* MWFLp-182 exhibited no cytotoxicity. *L. plantarum* MWFLp-182 and LGG showed auto-aggregation percentages of 89.39% and 70.82%, respectively, after 24 h (**Fig. 5A**). As shown in **Fig. 5B**, *L. plantarum* MWFLp-182 and LGG co-aggregated with *Salmonella* with co-aggregation percentages of 56.2% and 43.91%, respectively. After simulation of gastrointestinal juices, the survival rates of *L. plantarum* MWFLp-182 and LGG were 89.45% and 75.7%, respectively (**Table 2)**.

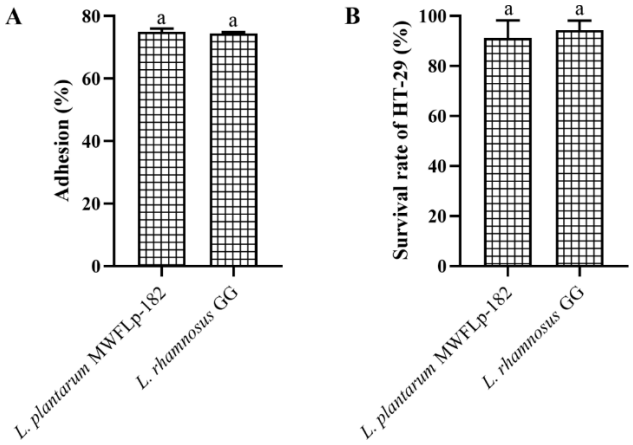

Fig. 4. LAB cell cytotoxicity (A) and adhesion capacity (B) to HT-29 cells.

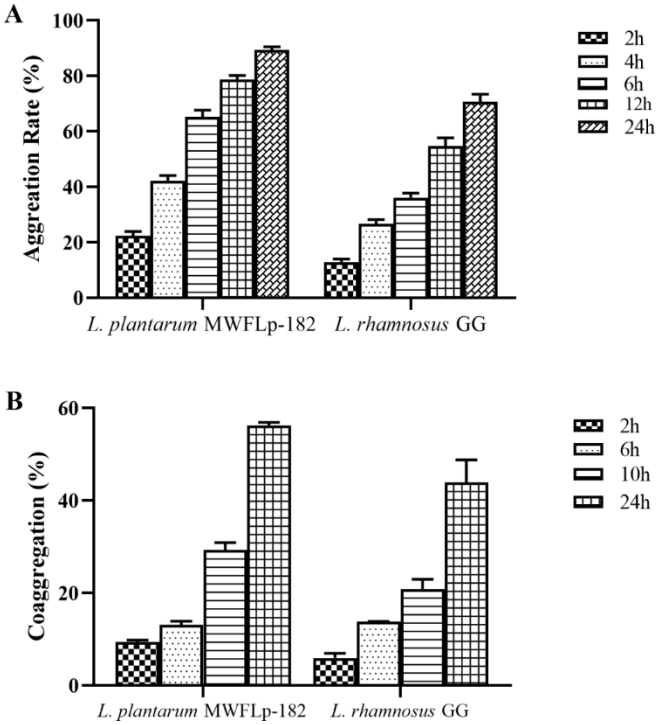

Fig. 5. Aggregation (A) and coaggregation rate (B) of *L. plantarum* MWFLp-182 and LGG.

Table 2. Gastrointesinal tolerance.

Name	Gastic juice (%)	Intestinal juice (%)
L. plantarum MWFLp-182	96.8 ± 1.2	89.45 ± 8.9
L. rhamnosus GG	86.6 ± 3.1	75.7 ± 2.3

3.4. Identification of genes implicated in the probiotic potential of L. plantarum MWFLp-182

We analyzed the genes involved in bile salt resistance, adhesion, nutritional synthesis, and cholesterol-lowering effects using the genomic data from *L. plantarum* MWFLp-182 (**Table 3**). The databases showed that *L. plantarum* MWFLp-182 contains 11 genes related to bile salt resistance; 7 genes related to adhesion; one gene related to the cholesterol-lowering effect; 1 gene related to nutritional synthesis; and 10 genes related to oxidative stress tolerance. Genes encoding the resistome and transferable antibiotic resistance genes from the ResFinder and Disinfinder databases were not found in *L. plantarum* MWFLp-182.

3.5 Protection of L. plantarum MWFLp-182 for HT-29 cells against ABAP injury

3.5.1 ROS production of HT-29 cells by L. plantarum MWFLp-182 treatment

ROS production aids the maintenance of a balance in normal cells; howener, oxidative stress increases ROS accumulation, and is the cause of damage to human body[38]. The intracellular ROS content was evaluated using the signal after the fluorescein-labeled dye of cells by DCFH-DA[39]. As shown in **Fig. 6**, the green fluorescence represents the ROS content. HT-29 cells were damaged after treatment with ABAP, which increased the fluorescence intensity. The fluorescence of *L. plantarum* MWFLp-182 and LGG treated HT-29 cells was lower than that of ABAP treated HT-29 cells. Thus, *L. plantarum* MWFLp-182 and LGG reduced the damage caused by oxidative stress in cells, and *L. plantarum* MWFLp-182 was more effective than was LGG.

Table 3. Potential genes associated with probiotic characteristics and oxidative stress tolerance from *L. plantarum* MWFLp-182.

Putative function	Gene ID	Gene name	Length (bp)	Product
Bile salt resistance		*yxel*	1017	Choloylglycine hydrolase family protein
		yiaC	444	GNAT family *N*-acetyltransferase
		elaA	444	GNAT family *N*-acetyltransferase
		rimJ	546	GNAT family *N*-acetyltransferase
		paiA	528	GNAT family *N*-acetyltransferase
		yjaB	468	GNAT family *N*-acetyltransferase
	gene0059	*rimL*	555	GNAT family *N*-acetyltransferase
	gene0267	*dnaK*	1869	Molecular chaperone DnaK
	gene0823	*dnaJ*	1143	Molecular chaperone DnaJ
	gene1155	*glmU*	1383	Bifunctional UDP-N-acetylglucosamine
	gene1506	*gadB*	1410	diphosphorylase/glucosamine-1-phosphate
Adhesion	gene1610	*srtA*	705	N-acetyltransferase
	gene2031	*dltD*	1278	Glutamate decarboxylase
	gene1657	*dltA*	1527	Class A sortase
	gene1656	*lspA*	450	*D*-Alanyl-lipoteichoic acid biosynthesis
	gene0398	*tuf*	1188	protein DltD
	gene2890	*gapA*	1023	*D*-Alanylation of LTA
	gene0419	*groEL*	1626	Lipoprotein signal peptidase
Cholesterol-lowering	gene1650	*cbh*	975	Elongation factor Tu
effect	gene1653	*lacI*	1011	Type I glyceraldehyde-3-phosphate
Nutritional synthesis	gene1467	*tpx*	609	dehydrogenase
Oxidative stress tolerance	gene1798	*trxA*	333	Chaperonin GroEL
	gene0623	*trxA*	312	Choloylglycine hydrolase
	gene0566	*trxA*	321	Catabolite control protein A
	gene2980	*trxB*	939	Thiol peroxidase
	gene1941	*npr*	1317	Thioredoxin
	gene1994	*npr*	1356	Thioredoxin
	gene0201	*nrdH*	231	Thioredoxin family protein
	gene1954	*dps*	468	Thioredoxin-disulfide reductase
	gene2909	*recA*	1143	FAD-dependent oxidoreductase
	gene2909	*gpx*	486	FAD-dependent oxidoreductase
	gene1204	*gshA*	2256	Redoxin NrdH
	gene2182	*arsC*	426	DNA starvation/stationary phase protection
	gene0538			protein
	gene2667			Recombinase RecA
	gene1976			GPx
	gene0189			Bifunctional glutamate-cysteine ligase
	gene2012			GshA/glutathione synthetase GshB
	gene0053			Arsenate reductase (thioredoxin)

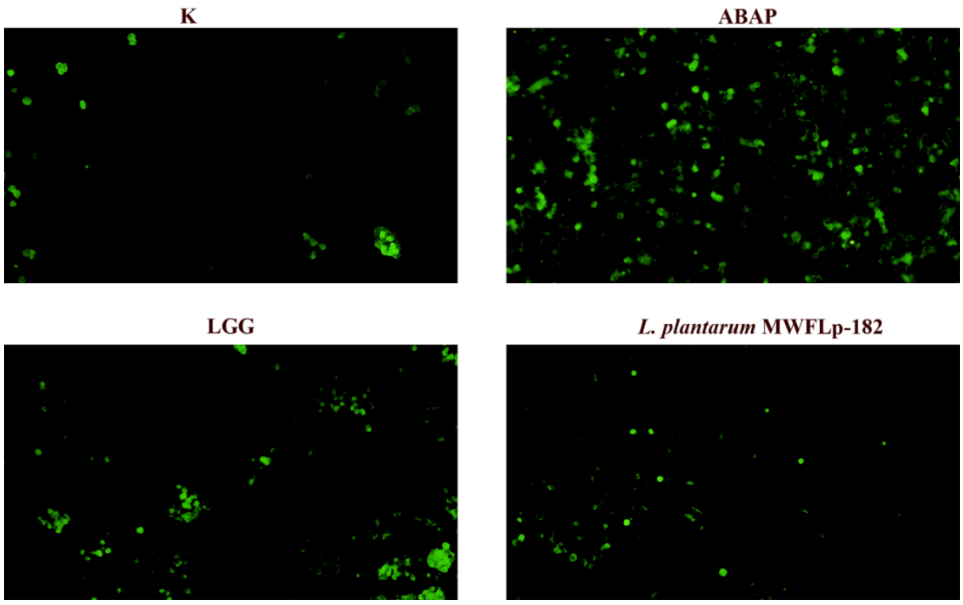

Fig. 6. Effects of pretreatment of *L. plantarum* MWFLp-182 and LGG on the ROS levels of ABAP induced HT-29 cells by fluorescent microscope (20×).

3.5.2 Analysis of mRNA expression in HT-29 cells

The expression of TJ, inflammatory, and oxidative cytokines was investigated to evaluate the effects of *L. plantarum* MWFLp-182 on ABAP-stimulated HT-29 cells (**Fig. 7**). Compared with the normal group (K), the ABAP-stimulated group could promote ($P < 0.05$) the expression of proinflammatory factors (*IL-1β* and *IL-6*) and *MDA*. Addition of *L. plantarum* MWFLp-182 resulted in significantly downregulated ($P < 0.05$) expression of *IL-6*, *IL-1β*, and *MDA* and significantly upregulated ($P < 0.05$) expression of *SOD3*, *GPx*, *IL-10*, *Nrf2*, *HO-1*, *Bcl-2*, *ZO-1*, *Claudin-1*, and *Occludin* in ABAP-damaged HT-29 cells, indicating that the damage symptoms induced by ABAP were effectively alleviated. These results indicated that *L. plantarum* MWFLp-182 relieved inflammation, oxidative stress, and gut barrier damage in ABAP-damaged HT-29 cells. Genes and primers selected for RT-qPCR were shown in **Table 4**.

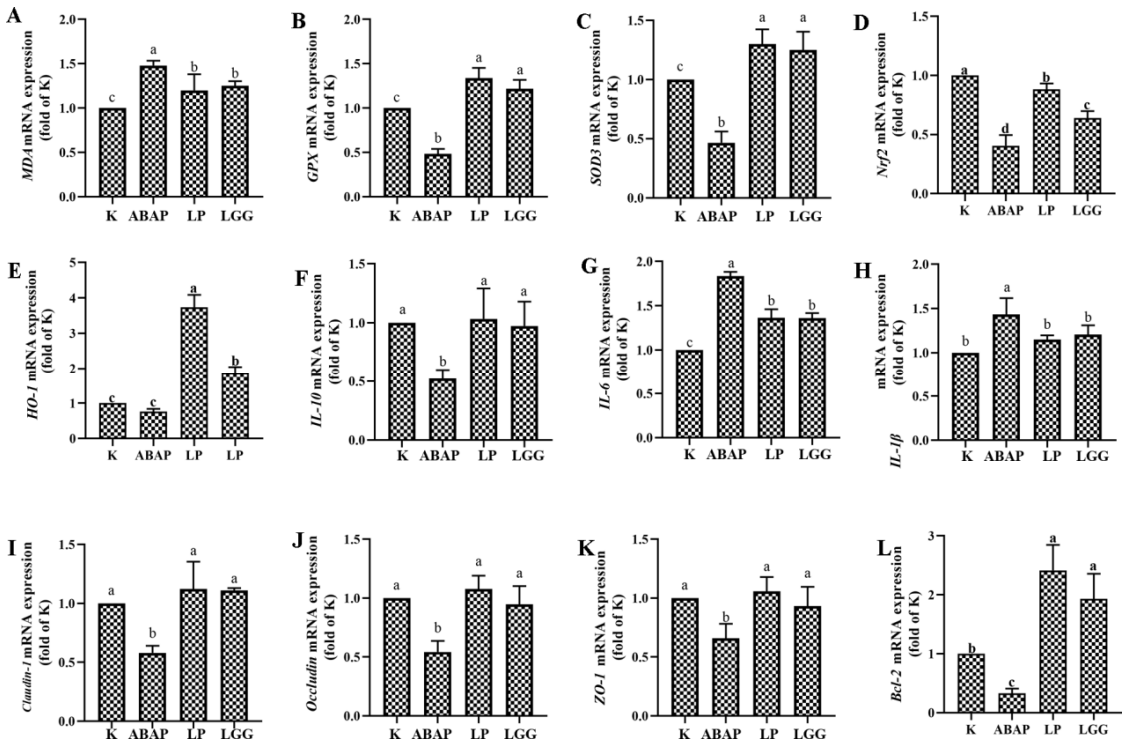

Fig. 7. Effects of *L. plantarum* MWFLp-182 on the *MDA* (A), *GPx* (B), *SOD3* (C), *Nrf2* (D), *HO-1* (E), *IL-10* (F), *IL-6* (G), *IL-1β* (H), *Claudin-1* (I), *Occludin* (J), *ZO-1* (K), and *Bcl-2* (L) expression of HT-29 cells. LGG was used as the positive control. Data are presented as mean ± SD. Different lowercase letters (a–c) show significant difference compared with the control ($P < 0.05$), as determined by one-way ANOVA. The same below.

Table 4. Genes and primers selected for RT-qPCR.

Gene	Primer	Sequence (5' to 3')
SOD3	Forward	ACGCTGGCGAGGACGACCTG
	Reverse	GCTTCTTGCGCTCTGAGTGCTC
MDA	Forward	AGGTGGACCTGGAGACTCTCAG
	Reverse	TCCTCTTGGAGAAGATCAGCCG
GPX	Forward	CGGCCCAGTCGGTGTATGC
	Reverse	CGTGGTGCCTCAGAGGGAC
IL-10	Forward	GACTTTAAGGGTTACCTGGGTTG
	Reverse	TCACATGCGCCTTGATGTCTG
IL-6	Forward	ACTCACCTCTTCAGAACGAATTG
	Reverse	CCATCTTTGGAAGGTTCAGGTTG
IL-1β	Forward	ATGATGGCTTATTACAGTGGCAA
	Reverse	GTCGGAGATTCGTAGCTGGA
Nrf2	Forward	GAGAGCCCAGTCTTCATTGC
	Reverse	ACTGGTTGGGGTCTTCTGTG
HO-1	Forward	TCAGGCAGAGGGTGATAGAA
	Reverse	GCTCCTGCAACTCCTCAAA
ZO-1	Forward	TTCACGCAGTTACGAGCAAG
	Reverse	TTGGTGTTTGAAGGCAGAGC
Occludin	Forward	GGGCATTGCTCATCCTGAAG
	Reverse	GCCTGTAAGGAGGTGTGACTT
Claudin-1	Forward	GGCCCTGCCATCTTTATTGG
	Reverse	ATTCCCAGGACAGGAACAGG
Bcl-2	Forward	AGATGTCCAGCCAGCTGCAC
	Reverse	TGTTGACTTCACTTGTGGCC
GAPHD	Forward	GGAAGGTGAAGGTCGGAGTC
	Reverse	TCAGCCTTGACGGTGCCATG

3.5.3 Analysis of protein expression in HT-29 cells

To clarify the mechanism underlying gut barrier damage, the regulatory effects of the ZO-1, Claudin-1 and Occludin signaling pathways were investigated in HT-29 cells. The survival rate of ABAP-stimulated (110 mmol/L) HT-29 cells was 50%. As shown in **Fig. 8**, compared with the control group (C), the expression of the TJ proteins ZO-1, Claudin-1 and Occludin was significantly reduced in the ABAP group. Importantly, *L. plantarum* MWFLp-182 significantly alleviated the decrease in the levels of TJ protein ZO-1, Claudin-1 and Occludin ($P < 0.05$).

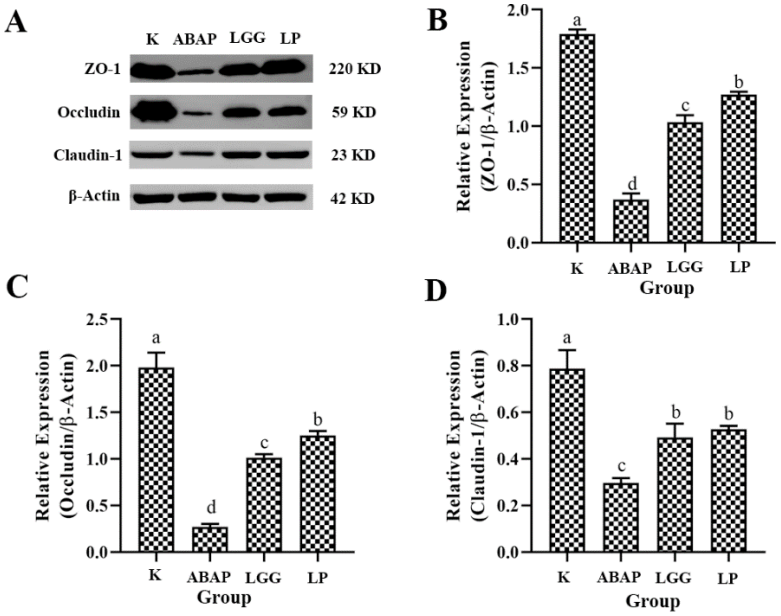

Fig. 8. Effects of *L. plantarum* MWFLp-182 and LGG on the expression of ZO-1 (B), Occludin (C), and Claudin-1 (D) in the SN of HT-29 cells. Protein bands were shown in (A).

4. Discussion

Probiotics have been known to be widespread in the gastrointestinal tract of long-living elderly individuals[40-41]; these probiotics include varied species such as *Lactobacillus*[40,42] and *Bifidobacterium* species[43-44], which have various benefits such as antioxidant, and improvement of learning and cognitive function[45]. In this study, strain MWFLp-182 was originally isolated from feces of long-living elderly individuals in Hezhou city, Guangxi, China, and whole-genome analysis was performed.

Probiotics play a role in protecting the host and must survive in the gastrointestinal environment[46]. *L. plantarum* MWFLp-182 exhibited stronger tolerance to simulated gastrointestinal juices, and we hypothesized that this was related to bile salt resistance genes. *L. plantarum* LM14-2 has adhesion genes (*rtA, dltD, dltA, lspA, and tuf*), and because of these, it showed an excellent adhesion ability to Caco-2 cells[31]; moreover, *L. plantarum* MWFLp-182 harbors similar genes. Auto-aggregation and co-aggregation abilities are important properties of probiotics that prevent infection by pathogenic microorganisms and protect the host[47-48]. *L. plantarum* KX519413 and KX519414 were isolated from the honey bee gut and exhibited co-aggregation with Salmonella (45.3%−63.6%), the ability to prevent colonization by pathogenic bacteria, and high auto-aggregation (99.26%−99.8%)[49]. *L. plantarum* MWFLp-182 displayed a co-aggregation rate of 56.2% with Salmonella, and an auto-aggregation rate of 89.39% after 24 h. Our results are similar to those of

a previous study; hence, *L. plantarum* MWFLp-182 protects the human body by preventing colonization by pathogenic bacteria.

Excessive ROS levels lead to aging by destroying lipids, proteins, and DNA[50]. During mitochondrial electron transport, electrons are transferred from ROS to O_2, and part of the O_2 is reduced to O^{2-} or H_2O_2. O_2 is converted to H_2O_2 by SOD, and H_2O_2 is then degraded to H_2O and O_2 by GPx[50]. ABAP can diffuse into cells and spontaneously decompose to form ROS[51]. As shown in **Fig. 6**, the levels of ROS in the ABAP group were higher than those in the control group, whereas after HT-29 cells were treated with *L. plantarum* MWFLp-182, the ROS levels were downregulated. This indicated that *L. plantarum* MWFLp-182 can relieve ABAP-stimulated damage in HT-29 cells.

SOD and GPx are important antioxidant enzymes that protect tissues from oxidative damage[52]. MDA is cytotoxic and an important product of membrane lipid peroxidation. LAB regulate antioxidant enzymes to relieve oxidative stress in host cells. *Lactobacillus plantarum* J26 protects Caco-2 cells against H_2O_2-induced oxidative damage by regulating SOD and GPx activities[53]. *L. acidophilus* La5 and *Bifidobacterium lactis* Bb12 can improve erythrocyte SOD and GPx activities in individuals with type 2 diabetes[54]. *B. bifidum* BGN4-SK treatment increases the levels of SOD and GPx in a lipopolysaccharide (LPS)-stimulated HT-29 cell model[55]. The surface layer proteins of *Lactoacillus* strains improved SOD activity and decreased MDA levels, in H_2O_2-stimulated HT-29 cells[56]. If the tissue is damaged, the inflammatory response is triggered as a defense mechanism against risk stimuli in the body and restores normal tissues[57]. A survey of available research showed that *L. pentosus* SMB718 exhibited antioxidant and anti-inflammatory activity in LPS-induced Caco-2 and HT-29 cells[58]; *L. plantarum* Y44 promoted expression of Nrf2 and TJ proteins, and downregulated expression of IL-8, TNF-α cytokines in ABAP-damaged Caco-2 cells[13]. Orlando et al.[59] reported that *L. rhamnosus* GG increases the expression of intercellular junction proteins at celiac disease.

Nrf2 can maintain cell redox homeostasis, if the level of intracellular ROS, Nrf2 will protect cells by activating the expression of antioxidant genes (*HO-1*, *GPx*, *SOD*) and anti-inflammatory genes[60]. Bcl-2 overexpression could inhibit lipid peroxidation and pro-oxidant effect of Bax, thereby preventing apoptosis. Meanwhile, Bcl-2 could eliminate intracellular ROS by upregulate SOD and GPx activities[61]. In our study, we found that after HT-29 cells were subjected to treatment with 110 μmol/L ABAP for 2 h, the expression of anti-inflammatory factor (IL-10), antioxidant cytokines (SOD, GPx, Nrf2, and HO-1), Bcl-2, and TJ proteins and genes (ZO-1, Claudin-1, and Occludin) were upregulated, while MDA and proinflammatory factor (IL-6, IL-1β, and TNF-α) expressions were reduced in ABAP-damaged HT-29 cells pretreated with *L. plantarum* MWFLp-182. In summary, all results suggested that *L. plantarum* MWFLp-182 can activity Nrf2/HO-1 antioxidant pathway, upregulate SOD, GPx, Nrf2, HO-1, and IL-10; downregulate MDA, IL-6, and IL-1β alleviate the oxidative stress and inflammation response of the ABAP-induced HT-29 cells injury. Meanwhile, *L. plantarum* MWFLp-182 can enhance Bcl-2 overexpression to upregulate SOD and GPx.

In addition, *L. plantarum* FLPL05 has an antioxidant system (glutathione and thioredoxin) with antioxidant capacity[14]; however, *L. plantarum* MWFLp-182 has a similar antioxidant system and antioxidant

genes, including *trxA*, *trxB*, *gpx*, *gshA* and *arsC.* Therefore, *L. plantarum* MWFLp-182 possesses antioxidant and anti-inflammatory properties.

5. Conclusions

In this study, *L. plantarum* MWFLp-182, isolated from the feces of long-living elderly individuals in Hezhou city, Guangxi, China, was found to have 11 bile salt resistance genes, seven adhesion genes, and no transferable antibiotic resistance genes. *L. plantarum* MWFLp-182 possessed a great ability to tolerate simulated gastrointestinal juices, and it grew well at pH 2 for 4 h. *L. plantarum* MWFLp-182 showed antioxidant and anti-inflammatory activity and enhanced, the expression of anti-inflammatory factors (IL-10), antioxidant cytokines (SOD, GPx), Bcl-2, and TJ proteins and their genes. Therefore, our research promotes the development of antioxidant strains and provides data and theoretical support for the high-throughput sequencing screening of antioxidant bacteria.

Declaration of competing interest

The authors declare that they have no known competing financial interests or personal relationships that could have appeared to influence the work reported in this paper.

Acknowledgements

This project was supported by the Natural Science Foundation of Guangxi, China (2020GXNSFBA297083) and the National Natural Science Foundation of China (32072193).

Reference

[1] E. Biagi, C. Franceschi, S. Rampelli, et al., Gut microbiota and extreme longevity, Curr. Biol. 26 (2016) 1480-1485. https://doi.org/10.1016/j.cub.2016.04.016.

[2] V. Mishra, C. Shah, N. Mokashe, et al., Probiotics as potential antioxidants: a systematic review, J. Agric. Food Chem. 63 (2015) 3615-3626. https://doi.org/10.1021/jf506326t.

[3] D. Cai, S.C. Zhao, D.L, Li, et al., Nutrient intake is associated with longevity characterization by metabolites and element profiles of healthy centenarians, Nutrients 8 (2016) 2-19. https://doi.org/10.3390/nu8090564.

[4] H.E. Seifried, D.E. Anderson, E.I. Fisher, et al., A review of the interaction among dietary antioxidants and reactive oxygen species, J. Nutr. Biochem. 18 (2007) 567-579. https://doi.org/10.1016/j.jnutbio.2006.10.007.

[5] M. Valko, D. Leibfritz, J. Moncol, et al., Free radicals and antioxidants in normal physiological functions and human disease, Int. J. Biochem. Cell Biol. 39 (2007) 44-84. https://doi.org/10.1016/j.biocel.2006.07.001.

[6] E.C. Ale, M.F. Rojas, J.A. Reinheimer, et al., *Lactobacillus fermentum*: could EPS production ability be responsible for functional properties?, Food Microbiol. 90 (2020) 103465. https://doi.org/10.1016/j.fm.2020.103465.

[7] M. Kumari, H.K. Patel, A. Kokkiligadda, et al., Characterization of probiotic lactobacilli and development of fermented soymilk with improved technological properties, LWT-Food Sci. Technol. 154 (2022) 112827. https://doi.org/10.1016/j.lwt.2021.112827.

[8] D.M. Liu, Y.Y. Huang, M.H. Liang, et al., Analysis of the probiotic characteristics and adaptability of *Lactiplantibacillus plantarum* DMDL 9010 to gastrointestinal environment by complete genome sequencing and corresponding phenotypes, LWT-Food Sci. Technol. 158 (2022) 113129. https://doi.org/10.1016/j.lwt.2022.113129.

[9] E.D. Kim, H.S. Lee, K.T. Kim, et al., Antioxidant and angiotensin-converting enzyme (ACE) inhibitory activities of yogurt supplemented with *Lactiplantibacillus plantarum* NK181 and *Lactobacillus delbrueckii* KU200171 and sensory evaluation, Foods 10 (2021) 2324. https://doi.org/10.3390/foods10102324.

[10] P. Khatantuul, L. Leona, D. Andrea, et al., The impact of cell-free supernatants of *Lactococcus lactis* subsp. *lactis* strains on the tyramine formation of *Lactobacillus* and *Lactiplantibacillus* strains isolated from cheese and beer, Food Microbiol. 99 (2021) 103813. https://doi.org/ 10.1016/j.fm.2021.103813.

[11] C. Liang, X.H. Zhou, P.M. Gong, et al., *Lactiplantibacillus plantarum* H-87 prevents high-fat diet-induced obesity by regulating bile acid metabolism in C57BL/6J mice, Food Funct. 10 (2021) 4315-4324. https://doi.org/10.1039/d1fo00260k.

[12] Q.Q. Zhou, R.C. Gu, P. Li, et al., Anti-*Salmonella* mode of action of natural *L*-phenyl lactic acid purified from *Lactobacillus plantarum* ZJ316, Appl. Microbiol. Biot. 104 (2020) 5283-5292. https://doi.org/10.1007/s00253-020-10503-4.

[13] G.Q. Mu, H.Y. Li, Y.F. Tuo, Antioxidative effect of *Lactobacillus plantarum* Y44 on 2,2′-azobis (2-methylpropionamidine) dihydrochloride (ABAP)-damaged Caco-2 cells, J. Dairy Sci. 102 (2019) 6863-6875. https://doi.org/10.3168/jds.2019-16447.

[14] X.M. Yu, Y.J. Li, Q.L. Wu, et al., Genomic analysis for antioxidant property of *Lactobacillus plantarum* FLPL05 from Chinese longevity people, Probiotics Antimicro. 12 (2020) 1451-1458. https://doi.org/10.1007/s12602-020-09704-0.

[15] A. Vetuschi, N. Battista, S. Pompili, et al., The antiinflammatory and antifibrotic effect of olive phenols and *Lactiplantibacillus plantarum* IMC513 in dextran sodium sulfate-induced chronic colitis, Nutrition 94 (2022) 111511. https://doi.org/10.1016/j.nut.2021.111511.

[16] J.S. Liu, X.F. Li, F.F. Song, et al., Dietary supplementation with low-dose xylooligosaccharide promotes the anti-*Salmonella* activity of probiotic *Lactiplantibacillus plantarum* ZS2058 in a murine model, Food Res. Int. 151 (2022) 110858. https://doi.org/10.1016/j.foodres.2021.110858.

[17] N. Adriana, Z.S. Małgorzata, R.K. Justyna, et al., Anticancer potential of post-fermentation media and cell extracts of probiotic strains: an *in vitro* study, Cancers 7 (2022) 1853. https://doi.org/10.3390/cancers14071853.

[18] Y.G. Gu, J. Bai, J.Y. Zhang, et al., *Lactiplantibacillus plantarum* fermented barley extracts ameliorate HFD-induced muscle dysfunction via mitophagy, J. Sci. Food Agric. 102 (2022) 5261-5271. https://doi.org/10.1002/jsfa.11879.

[19] Y. Gao, Y.J. Liu, M.Y. Sun, et al., Physiological function analysis of *Lactobacillus plantarum* Y44 based on genotypic and phenotypic characteristics, J. Dairy Sci. 103 (2020) 5916-5930. https://doi.org/10.3168/jds.2019-18047.

[20] J. Wang, H.F. Ji, S.X. Wang, et al., Probiotic *Lactobacillus plantarum* promotes intestinal barrier function by strengthening the epithelium and modulating gut microbiota, Front. Microbio. 9 (2018) 1953. https://doi.org/10.3389/fmicb.2018.01953.

[21] L.J. Zhang, Y. Meng, J.Y. Li, et al., *Lactiplantibacillus plantarum* Y42 in biofilm and planktonic states improves intestinal barrier integrity and modulates gut microbiota of BALB/c mice, Foods 11 (2022) 1451. https://doi.org/10.3390/foods11101451.

[22] A.E. Yetiman, A. Keskin, B.N. Darendeli, et al., Characterization of genomic, physiological, and probiotic features *Lactiplantibacillus plantarum* DY46 strain isolated from traditional lactic acid fermented shalgam beverage, Food Biosci. 46 (2022) 101499. https://doi.org/10.1016/j.fbio.2021.101499.

[23] B.Y. Mao, R.M. Yin, X.S. Li, et al., Comparative genomic analysis of *Lactiplantibacillus plantarum* isolated from different Niches, Genes 12 (2021) 241. https://doi.org/10.3390/genes12020241.

[24] L. Axelsson, I. Rud, K. Naterstad, et al., Genome sequence of the naturally plasmid-free *Lactobacillus plantarum* strain NC8 (CCUG 61730), J. Bacteriol. 194 (2012) 2391-2392.

[25] Y.J. Wang, H.Y. Yang, G.Q. Mu, et al., Safety evaluation and complete genome analysis emphasis on extracellular polysaccharide of two strains of *Limosilactobacillus fermentum* MWLf-4 and *Lactipiantibacillus plantarum* MWLp-12 from human milk, Food Biosci. 51 (2023) 102356. https://doi.org/10.1016/j.fbio.2023.102356.

[26] P.K. Montso, C.C. Bezuidenhout, C. Mienie, et al., Genetic diversity and whole genome sequence analysis data of multidrug resistant atypical enteropathogenic *Escherichia coli* O177 strains: an assessment of food safety and public health implications, Int. J. Food Microbiol. 365 (2022) 109555. https://doi.org/10.1016/j.ijfoodmicro.2022.109555.

[27] S. Koren, B.P. Walenz, K. Berlin, et al., Canu: scalable and accurate long-read assembly via adaptive *k*-mer weighting and repeat separation, Genome Res. (2017) 215087. https://doi.org/10.1101/gr.215087.116.

[28] A.L. Delcher, K.A. Bratke, E.C. Powers, et al., Identifying bacterial genes and endosymbiont DNA with Glimmer, Bioinformatics 23 (2007) 673-679. https://doi.org/10.1093/bioinformatics/btm009.

[29] W. Zhang, H.F. Ji, D.Y. Zhang, et al., Complete genome sequencing of *Lactobacillus plantarum* ZLP001, a potential probiotic that enhances intestinal epithelial barrier function and defense against pathogens in pigs, Front. Physiol. 9 (2018) 1689. https://doi.org/10.3389/fphys.2018.01689.

[30] C. Liu, W.J. Xue, H. Ding, et al., Lactobacillus probiotic potential of strains isolated from fermented vegetables in Shaanxi, China, Front. Microbio. 12 (2021) 774903. https://doi.org/10.3389/fmicb.2021.774903.

[31] E. Kingkaew, H. Konno, Y. Hosaka, et al., Probiogenomic analysis of *Lactiplantibacillus* sp. LM14-2 from fermented Mussel (*Hoi-dong*), and evaluation of its cholesterol-lowering and immunomodulation effects, Probiotics Antimicro. 15 (2022) 1206-1220. https://doi.org/10.1007/s12602-022-09977-7.

[32] J. Xing, G. Wang, Z. Gu, et al., Cellular model to assess the antioxidant activity of lactobacilli, RSC Adv. 5 (2015) 37626-37634. https://doi.org/10.1039/C5RA02215K.

[33] S. Plessas, D.E. Kiousi, M. Rathosi, et al., Isolation of a *Lactobacillus paracasei* strain with probiotic attributes from kefir grains, Biomedicines 8 (2020) 594. https://doi.org/10.3390/biomedicines8120594.

[34] L.Y. Xiao, X.J. Ge, L. Yang, et al., Anticancer potential of exopolysaccharide from *Lactobacillus helveticus* MB2-1 on human colon cancer HT-29 cell via apoptosis induction, Food Funct. 11 (2020) 10170-10181. https://doi.org/10.1039/d0fo01345e.

[35] F.L. Ma, Y.L. Song, M.Y. Sun, et al., Exopolysaccharide produced by *Lactiplantibacillus plantarum*-12 alleviates intestinal inflammation and colon cancer symptoms by modulating the gut microbiome and metabolites of C57BL/6 mice treated by Azoxymethane/Dextran sulfate sodium salt, Foods 10 (2021) 3060. https://doi.org/10.3390/foods10123060.

[36] K.J. Lo, S.S. Lin, C.W. Lu, et al., Whole-genome sequencing and comparative analysis of two plant-associated strains of *Rhodopseudomonas palustris* (PS3 and YSC3), Sci. Rep. 8 (2018) 12769. https://doi.org/10.1038/s41598-018-31128-8.

[37] L. Cai, S.W. Zheng, Y.J. Shen, et al., Complete genome sequence provides insights into the biodrying-related microbial function of *Bacillus thermoamylovorans* isolated from sewage sludge biodrying material, Bioresource Technol. 260 (2018) 141-149. https://doi.org/10.1016/j.biortech.2018.03.121.

[38] X.M. Yu, X.L. Wu, N.P. Shah, et al., Interaction between *Bifidobacterium bifidum* and *Listeria monocytogenes* enhances antioxidant activity through oxidoreductase system, LWT-Food Sci. Technol. 127 (2020) 109209. https://doi.org/10.1016/j.lwt.2020.109209.

[39] C. Messaoud, A. Laabidi, M. Boussaid, *Myrtus communis* L. infusions: the effect of infusion time on phytochemical composition, antioxidant, and antimicrobial activities, J. Food Sci. 77 (2012) C1-C7. https://doi.org/10.1111/j.1750-3841.2012.02849.x.

[40] Y. Li, J. Gao, L. Xue, et al., *Limosilactobacillus fermentum* determination of antiviral mechanism of centenarian gut-derived against norovirus, Front. Nutr. 9 (2022) 812623. https://doi.org/ 10.3389/fnut.2022.812623.

[41] M. Deng, X. Wu, X. Duan, et al., *Lactobacillus paracasei* L9 improves colitis by expanding butyrate-producing bacteria that inhibit the IL-6/STAT3 signaling pathway, Food Funct. 12 (2021) 10700-10713. https://doi.org/10.1039/d1fo02077c.

[42] M.H. Ren, H. Li, Z. Fu, et al., Centenarian-sourced *Lactobacillus casei* combined with dietary fiber complex ameliorates brain and gut function in aged mice, Nutrients 14 (2022) 324. https://doi.org/10.3390/nu14020324.

[43] Y.L. Hao, D.W. Huang, H.Y. Guo, et al., Complete genome sequence of *Bifidobacterium longum* subsp. *Longum* BBMN68, a new strain from a healthy Chinese centenarian, J. Bacteriol. 193 (2011) 787-788. https://doi.org/10.1128/JB.01213-10.

[44] F. Wang, G.H. Huang, D. Cai, et al., Qualitative and semiquantitative analysis of fecal *Bifidobacterium* species in centenarians living in Bama, Guangxi, China, Curr. Microbiol. 71 (2015) 143-149. https://doi.org/10.1007/s00284-015-0804-z.

[45] Y. Ni, X. Yang, L. Zheng, et al., *Lactobacillus* and *Bifidobacterium* improves physiological function and cognitive ability in aged mice by the regulation of gut microbiota, Mol. Nutr. Food Res. 63 (2019) e1900603. https://doi.org/ 10.1002/mnfr.201900603.

[46] Q.Q. Zhou, N. Qureshi, B.Y. Xue, et al., Preventive and therapeutic effect of *Lactobacillus paracasei* ZFM54 on helicobacter pylori-induced gastritis by ameliorating inflammation and restoring gastric microbiota in mice model, Front. Nutr. 9 (2022) 972569. https://doi.org/10.3389/fnut.2022.972569.

[47] C. Dunne, B. Dolan, M. Clyne, Factors that mediate colonization of the human stomach by *Helicobacter pylori*, World J. Gastroenterol. 20 (2014) 5610-5624. https://doi.org/10.3748/wjg.v20.i19.5610.

[48] L. Merino, F.M. Trejo, G. de Antoni, et al., *Lactobacillus* strains inhibit biofilm formation of *Salmonella* sp. isolates from poultry, Food Res. Int. 123 (2019) 58-65. https://doi.org/10.1016/j.foodres.2019.04.067.

[49] C.C. Honey, T.R. Keerthi, Probiotic potency of *Lactobacillus plantarum* KX519413 and KX519414 isolated from honey bee gut, FEMS Microbiol. Lett. 365 (2018) 1-8. https://doi.org/10.1093/femsle/fnx285.

[50] J.Y. Zhang, P. Wang, C. Tan, et al., Integrated transcriptomics and metabolomics unravel the metabolic pathway variations for barley *β*-glucan before and after fermentation with *L. plantarum* DY-1, Food Funct. 13 (2022) 4302-4314. https://doi.org/10.1039/d1fo02450g.

[51] K.L. Wolfe, R.H. Liu, Cellular antioxidant activity (CAA) assay for assessing antioxidants, foods, and dietary supplements, J. Agric. Food Chem. 55 (2007) 8896-8907. https://doi.org/10.1021/jf0715166.

[52] S.S.K. Wijeratne, S.L. Cuppett, V. Schlegel, Hydrogen peroxide induced oxidative stress damage and antioxidant enzyme response in Caco-2 human colon cells, J. Agric. Food Chem. 53 (2005) 8768-8774. https://doi.org/10.1021/jf0512003.

[53] Y.C. Hou, X.S. Li, X.Y. Liu, et al., Transcriptomic responses of Caco-2 cells to *Lactobacillus rhamnosus* GG and *Lactobacillus plantarum* J26 against oxidative stress, J. Dairy Sci. 102 (2019) 7684-7696. https://doi.org/10.3168/jds.2019-16332.

[54] H.S. Ejtahed, J. Mohtadinia, A. Homayounirad, et al., Probiotic yogurt improves antioxidant status in type 2 diabetic patients, Nutrition 28 (2012) 539-543. https://doi.org/10.1016/j.nut.2011.08.013.

[55] S.N. Kang, Z.Y. Zhang, Y. Yu, et al., A recombinant *Bifidobacterium bifidum* BGN4 strain expressing the streptococcal superoxide dismutase gene ameliorates inflammatory bowel disease, Microb. Cell Fact. 21 (2022) 113. https://doi.org/10.1186/s12934-022-01840-2.

[56] B.B. Zhao, J. Meng, Q.X. Zhang, et al., Protective effect of surface layer proteins isolated from four *Lactobacillus* strains on hydrogen-peroxide-induced HT-29 cells oxidative stress, Int. J. Biol. Macromol. 102 (2017) 76-83. https://doi.org/10.1016/j.ijbiomac.2017.03.160

[57] K.J. Han, J.E. Lee, N.K. Lee, et al., Antioxidant and anti-inflammatory effect of probiotic *Lactobacillus plantarum* KU15149 derived from Korean homemade diced-radish kimchi, J. Microbiol. Biotechnol. 30 (2020) 591-598. https://doi.org/10.4014/jmb.2002.02052.

[58] Y.M. Jo, H. Seo, G.Y. Kim, et al., *Lactobacillus pentosus* SMB718 as a probiotic starter producing allyl mercaptan in garlic and onion-enriched fermentation, Food Funct. 11 (2021) 10913-10924. https://doi.org/10.1039/d0fo02000a.

[59] A. Orlando, M. Linsalata, G. Bianco, et al., *Lactobacillus rhamnosus* GG protects the epithelial barrier of Wistar rats from the pepsin-trypsin-digested gliadin (PTG)-induced enteropathy, Nutrients 10 (2018) 1698. https://doi.org/10.3390/nu10111698.

[60] S.J. Liu, Y. Zhao, X.W. Xu, et al., *Lactiplantibacillus plantarum* P101 alleviates alcoholic liver injury by modulating the Nrf2/HO-1 pathway in mice, J. Appl. Microbiol. 134 (2022) 1-10. https://doi.org/10.1093/jambio/lxac032.

[61] Y.H Lee, S.J.F. Chong, S. Pervaiz, The anti-oxidant and pro-oxidant dichotomy of Bcl-2, Biol. Chem. 397 (2016) 585-593. https://doi.org/10.1515/hsz-2016-0127